

# Concurrent approaches to Generalized Parton Distribution modeling: the pion's case

N. Chouika<sup>1</sup>, C. Mezrag<sup>2</sup>, H. Moutarde<sup>1,a</sup>, and J. Rodríguez-Quintero<sup>3</sup>

<sup>1</sup>IRFU, CEA, Université Paris-Saclay, F-91191 Gif-sur-Yvette, France

<sup>2</sup>Physics Division, Argonne National Laboratory, Argonne, Illinois 60439, USA

<sup>3</sup>Dpt. Física Aplicada, Fac. CCEE, Universidad de Huelva, Huelva E-21071, Spain

**Abstract.** The concept of Generalized Parton Distributions promises an understanding of the generation of the charge, spin, and energy-momentum structure of hadrons by quarks and gluons. Forthcoming measurements with unprecedented accuracy at Jefferson Lab and at CERN will challenge our quantitative description of the three-dimensional structure of hadrons. To fully exploit these future measurements, new tools and models are currently being developed.

We explain the difficulties of Generalized Parton Distribution modeling, and present some recent progresses. In particular we describe the symmetry-preserving Dyson-Schwinger and Bethe-Salpeter framework. We also discuss various equivalent parameterizations and sketch how to combine them to obtain models satisfying *a priori* all required theoretical constraints. At last we explain why these developments naturally fit in a versatile software framework, named PARTONS, dedicated to the theory and phenomenology of GPDs.

## 1 Introduction

Generalized Parton Distributions (GPDs) were introduced independently by Müller *et al.* [1], Ji [2] and Radyushkin [3]. They are related to hadron form factors and contain the usual Parton Distribution Functions (PDFs) as a limiting case. They constitute a unifying framework for these classical objects, and they also provide unique, new information about the structure of hadrons, including 3D imaging of their partonic content as recently reviewed in Ref. [4]. GPDs have been the object of a continuous theoretical, phenomenological and experimental activity (see the reviews [5–14] and references therein).

Most of the theoretical constraints (support property, discrete symmetries, polynomiality) on GPDs are fulfilled when GPDs are parameterized with Double Distributions (DDs) [1, 15, 16]. Formally it is equivalent to expressing GPDs as Radon transforms of DDs [17]. However there is no known first principle parameterization of GPDs fulfilling all theoretical constraints. For example, positivity and chiral symmetry –connecting a pion GPD to a pion Distribution Amplitude (DA)– usually evade DD parameterization. Therefore computing

---

<sup>a</sup>e-mail: herve.moutarde@cea.fr

GPDs in a symmetry-preserving framework is an essential ingredient to satisfy *a priori* all GPD theoretical requirements as detailed *e.g.* in Ref. [18].

Here we briefly summarize the theoretical aspects of GPDs, discuss the symmetry-preserving feature of Dyson-Schwinger and Bethe-Salpeter equations, present a generic procedure to extend an overlap of Light Front Wave Functions (LFWFs) from the DGLAP to the ERBL region, and describe how it naturally fits in the software framework PARTONS.

## 2 Theoretical framework

For a given 4-vector  $v$ , we define  $v^\pm = (v^0 \pm v^3)/\sqrt{2}$  and note  $v = (v^+, v_\perp, v^-)$ . For the sake of simplicity, we focus on the case of the chiral-even pion GPD  $H^q$  for a quark flavor  $q$ , defined by:

$$H^q(x, \xi, t) = \frac{1}{2} \int \frac{dz^-}{2\pi} e^{ixP^+z^-} \left\langle \pi, P + \frac{\Delta}{2} \left| \bar{q} \left( -\frac{z}{2} \right) \gamma^+ q \left( \frac{z}{2} \right) \right| \pi, P - \frac{\Delta}{2} \right\rangle_{\substack{z^+=0 \\ z_\perp=0}}, \quad (1)$$

with  $t = \Delta^2$  and  $\xi = -\Delta^+/(2P^+)$ . It can be easily read from this matrix element that:

1. The forward limit of the GPD is the PDF:  $H^q(x, 0, 0) = q(x)$ .
2. The integral over  $x$  of the GPD gives the quark contribution  $F_1^q$  to the form factor  $F_1$ :  $\int_{-1}^{+1} dx H^q(x, \xi, t) = F_1^q(t)$ .
3.  $H^q$  is an even function of  $\xi$  from time-reversal invariance.
4.  $H^q$  is real from hermiticity and time-reversal invariance.

However, some other properties are nontrivial:

**Polynomiality**  $\int_{-1}^{+1} dx x^m H^q(x, \xi, t)$  is a polynomial in  $\xi$  of degree at most  $m + 1$ . This statement stems from Lorentz covariance and discrete symmetries.

**Positivity**  $H^q(x, \xi, t)$  is bounded from above. This upper bounds depends on values of the corresponding PDF at special kinematics. It reflects the positivity of the norm in a Hilbert space.

**Support** The  $x$ -support of  $H^q$  is  $[-1, +1]$ . This holds true in a quantum relativistic framework.

**Soft pion theorem** It expresses the breaking of chiral symmetry. In the pion case, it relates the isovector pion GPD  $H^{I=1}(x, \xi = 0, t = 0)$  to the pion DA  $\phi((x + 1)/2)$ .

DDs are commonly regarded as a convenient way to deal with the polynomiality property. Introducing the two pion DDs  $F^q$  and  $G^q$ , denoting  $\Omega_{\text{DD}} = \{(\beta, \alpha) \in \mathbb{R}^2 / |\alpha| + |\beta| \leq 1\}$ , the relation:

$$H^q(x, \xi, t) = \int_{\Omega_{\text{DD}}} d\beta d\alpha \delta(x - \beta - \alpha\xi) (F^q(\beta, \alpha, t) + \xi G^q(\beta, \alpha, t)), \quad (2)$$

automatically fulfills the polynomiality condition (see Fig. 1). Then every GPD model built on DDs satisfies this property. What is often less emphasized is the fact that the polynomiality condition exactly means that a GPD lies in the image space of the Radon transform [19]. Therefore the polynomiality condition can be replaced by a study of the properties of the Radon transform *without loss of generality*.

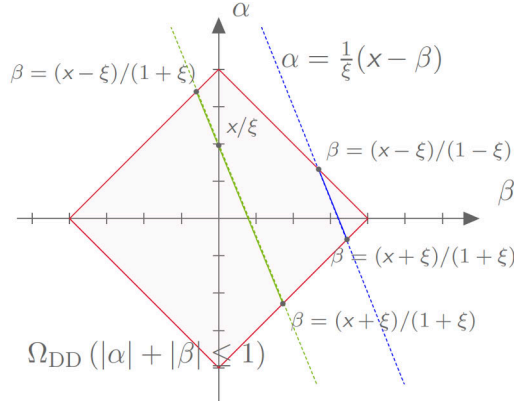


**Figure 1.** Integration lines defining a GPD at  $(x, \xi)$  in the  $(\beta, \alpha)$ -plane of DD variables.

The positivity property consists in infinitely many inequalities stable under Leading Order (LO) evolution [20] in the DGLAP region. The overlap representation [21] guarantees *a priori* the fulfillment of positivity constraints since this representation makes clear the underlying inner product structure of the considered Hilbert space. Generalizing the pioneering work of Refs. [22, 23], it is possible to systematically build GPD models starting from an expression of a GPD as an overlap of LFWFs in the DGLAP region, invert the Radon transform to get a DD, and from this DD covariantly extend the original GPD to the ERBL region.

### 3 Dyson-Schwinger and Bethe-Salpeter approach

We now illustrate this generic model-building procedure with a specific example. In Ref. [24] we showed how a consistent implementation of chiral symmetry in the pion Bethe-Salpeter and quark gap equations naturally leads, in a rainbow-ladder truncation, to a GPD model obeying the soft pion theorem. However for the sake of simplicity we will use here a simple and insightful algebraic model developed in an analog study of the pion DA [25] and also used to sketch features of the valence pion PDF and GPD [24, 26, 27]:

$$S(\ell) = [-i\gamma \cdot \ell + M]\Delta_M(\ell^2), \quad (3)$$

$$\rho_\nu(z) = \frac{1}{\sqrt{\pi}} \frac{\Gamma(\nu + 3/2)}{\Gamma(\nu + 1)} (1 - z^2)^\nu, \quad (4)$$

$$n_\pi \Gamma_\pi(\ell_\pm^R; \pm P) = i\gamma_5 \int_{-1}^1 dz \rho_\nu(z) \hat{\Delta}_M^\nu(\ell_{z\pm}^2), \quad (5)$$

for the dressed-quark and pion Bethe-Salpeter vertex. We use the following notations:  $\Delta_M(\ell^2) = 1/(\ell^2 + M^2)$  ( $M$  is a dressed quark mass),  $\hat{\Delta}_M(\ell^2) = M^2 \Delta_M(\ell^2)$ ;  $\ell_{z\pm} = \ell_\pm^R + (z \pm 1)P/2$ ,  $n_\pi$  is the canonical normalisation constant of the Bethe-Salpeter amplitude.

In the DGLAP region, the pion GPD  $H^q(x, \xi, t)$  can be represented as an overlap of LFWFs:

$$H^q(x, \xi, t)|_{\text{DGLAP}} = C^q \int d^2\mathbf{k}_\perp \Psi^* \left( \frac{x - \xi}{1 - \xi}, \mathbf{k}_\perp + \frac{1 - x}{1 - \xi} \frac{\Delta_\perp}{2}; P_- \right) \Psi \left( \frac{x + \xi}{1 + \xi}, \mathbf{k}_\perp - \frac{1 - x}{1 + \xi} \frac{\Delta_\perp}{2}; P_+ \right), \quad (6)$$

where  $C^q$  is a normalization constant. The LFWF  $\Psi$  can be computed by integrating over  $k^-$  the projection onto  $\gamma^+\gamma_5$  of the pion Bethe-Salpeter wave function  $\chi_\pi(k, P)$ :

$$\Psi(k^+, \mathbf{k}_\perp; P) = -\frac{1}{2\sqrt{3}} \int \frac{dk^-}{2\pi} \text{Tr}[\gamma^+\gamma_5 \chi_\pi(k, P)]. \quad (7)$$

We first use Eq. (7) to get a Bethe-Salpeter wave function from Eqs. (3)-(5), and subsequently plug it into Eq. (6). We are finally left with the corresponding DGLAP overlap GPD [18]:

$$H^u(x, \xi, 0)|_{\text{DGLAP}} = \mathcal{N}_v \frac{(1-x)^{2\nu}(x^2 - \xi^2)^\nu}{(1 - \xi^2)^{2\nu}}. \quad (8)$$

## 4 Extension: implementing positivity and polynomiality

### 4.1 Radon transform

For  $s > 0$  and  $\phi \in [0, 2\pi]$ , the Radon transform  $\mathcal{R}f$  of a function  $f$  is defined by (see Fig. 2):

$$\mathcal{R}f(s, \phi) = \int_{-\infty}^{+\infty} d\beta d\alpha f(\beta, \alpha) \delta(s - \beta \cos \phi - \alpha \sin \phi), \quad (9)$$

The redundancy in the  $s, \phi$  coverage is manifest in the symmetry property:

$$\mathcal{R}f(-s, \phi) = \mathcal{R}f(s, \phi \pm \pi). \quad (10)$$

The relation to GPDs and DDs is made through the following dictionary:

$$x = \frac{s}{\cos \phi}, \quad (11)$$

$$\xi = \tan \phi, \quad (12)$$

$$\frac{\sqrt{1 + \xi^2}}{x} H^q(x, \xi) = \mathcal{R}f_{\text{BMKS}}^q(s, \phi), \quad (13)$$

$$\frac{\sqrt{1 + \xi^2}}{1 - x} H^q(x, \xi) = \mathcal{R}f_{\text{P}}^q(s, \phi), \quad (14)$$

where the last two equations invoke special representations of DDs [11, 17, 28–30] (where the two DDs  $F^q$  and  $G^q$  are in fact related to one single function  $f^q$ ) yielding the same GPD. These physically equivalent representations can be mapped into each other by means of so-called *gauge* transformations.

The Radon transform has been thoroughly studied by mathematicians in connection with computerized tomography. It is possible to specify when the Radon transform can be inverted, characterizing solutions and their uniqueness properties under some smoothness and consistency conditions [31].

### 4.2 Covariant extension

We numerically invert the Radon transform by discretizing the DD support  $\Omega_{\text{DD}}$  and looking for a piecewise constant DD. Therefore we are left with a matrix inversion problem  $Ax = y$  in a large dimension space, the dimension being determined by the number of cells in the discretized DD support. The linear operator  $A$  expresses the action of the Radon transform

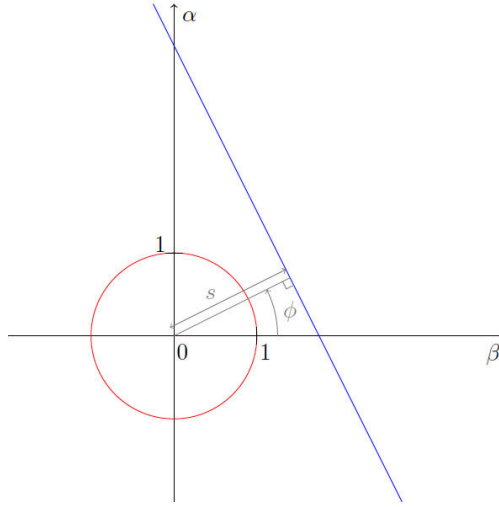


**Figure 2.** Polar coordinates used in the definition of the Radon transform in the usual  $(\beta, \alpha)$ -plane of DD variables. An integration line is defined by its (algebraic) distance  $s$  to the origin and the angle  $\phi$  between its normal and the abscissa axis.

on this discretized DD space. This is a *mildly ill-posed* problem because the inverse of the Radon transform is not continuous. Thus numerical noise may become prohibitively large, and much care is needed in the numerical resolution of this inverse problem. In our case, the DD solution has been constrained by implementing two physically-grounded properties:

1. The parity in  $\alpha$ :  $f^q(\beta, -\alpha) = f^q(\beta, \alpha)$ .
2. The restriction to valence-quark GPDs:  $f^q(\beta, \alpha) = 0$  for  $\beta < 0$ .

The  $\alpha$ -parity reduces the dimension of the matrix and requires a symmetrization of the discrete contributions coming from both sides of the  $\alpha = 0$  line. By linearity, the restriction to the  $\beta > 0$  part of the DD support does not reduce the generality of the approach. More details about this inverse problem, in particular concerning the numerical aspects, will be found in a forthcoming work [32].

We have successfully checked our numerical resolution with simple examples, as a constant DD over the restricted support where  $\beta > 0$ , and with a simplified version of the Radyushkin Double Distribution Ansatz (RDDA) [33]:

$$\left. \begin{array}{l} \text{P} \\ \text{BMKS} \end{array} \right\} (1-\beta) \left. \begin{array}{l} \\ \beta \end{array} \right\} \times f_{RDDA}^q(\beta, \alpha) = \frac{\Gamma(N+3/2)}{\sqrt{\pi}\Gamma(N+1)} \frac{[(1-|\beta|)^2 - \alpha^2]^N}{(1-|\beta|)^{2N+1}} q(\beta), \quad (15)$$

specialized to  $N = 1$  and to the simple PDF  $q(\beta) = \beta^2(1-\beta)^2$ . The corresponding GPD can be analytically computed in the DGLAP region, and the Radon transform numerically inverted to yield a DD. This reconstructed DD agrees very well with the original DD given by Eq. (15), as can be seen in Fig. 3.

The same numerical procedure has been applied to the overlap GPD given by Eq. (8). We found a much smoother solution by inverting the GPD expressed as a Radon transform in

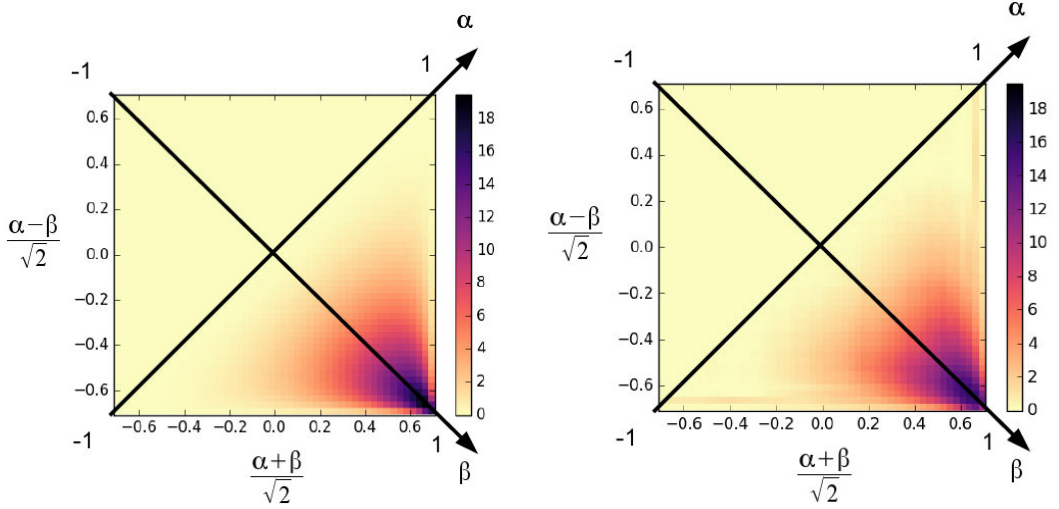


**Figure 3.** Left: Poblitsa-gauge DD for  $t = 0$  obtained from the analytical expression Eq. (15). Right: DD resulting of the numerical inverse Radon transform of the associated GPD restricted to the DGLAP region. The support for the parameters  $(\beta, \alpha)$  corresponds to a  $\pi/2$ -rotated square with the two combinations  $(\alpha + \beta)/\sqrt{2}$  and  $(\alpha - \beta)/\sqrt{2}$  for the horizontal and vertical axes.

the Poblitsa gauge Eq. (14) than in the BMKS gauge Eq. (13). From the numerical solution in the Poblitsa gauge, it was possible to elaborate a polynomial Ansatz for the DD. Then by direct algebraic computations with this Ansatz we obtained an exact analytic solution to the inverse problem:

$$f_{\text{P}}(\beta, \alpha) = \frac{30}{4} (1 - 3\alpha^2 - 2\beta + 3\beta^2). \quad (16)$$

The agreement between the numerical result and the analytic result is very good (see Fig. 4). The mapping from the Poblitsa to the BMKS gauge can be easily computed [11] and we find:

$$f_{\text{BMKS}}(\beta, \alpha) = \frac{30}{4} \left( \alpha^2 \left( 3 - \frac{3}{(|\alpha| + \beta)^3} \right) + (3\beta^2 - 4\beta) \left( \frac{1}{(|\alpha| + \beta)^4} - 1 \right) + \frac{2}{(|\alpha| + \beta)^2} - 2 + (1 - \alpha^2)\delta(\beta) \right), \quad (17)$$

which exhibits a singular behavior on the  $\beta = 0$  line. This is precisely why the Poblitsa gauge appears to be the most appropriate gauge for the inversion of the Radon transform in this example. However this is presumably a generic feature that could be expected from other models.

## 5 PARTONS project

The lack of a general first principles parameterization of GPDs justifies the use of several models for phenomenological studies. As seen above, the complexity of GPD model-building

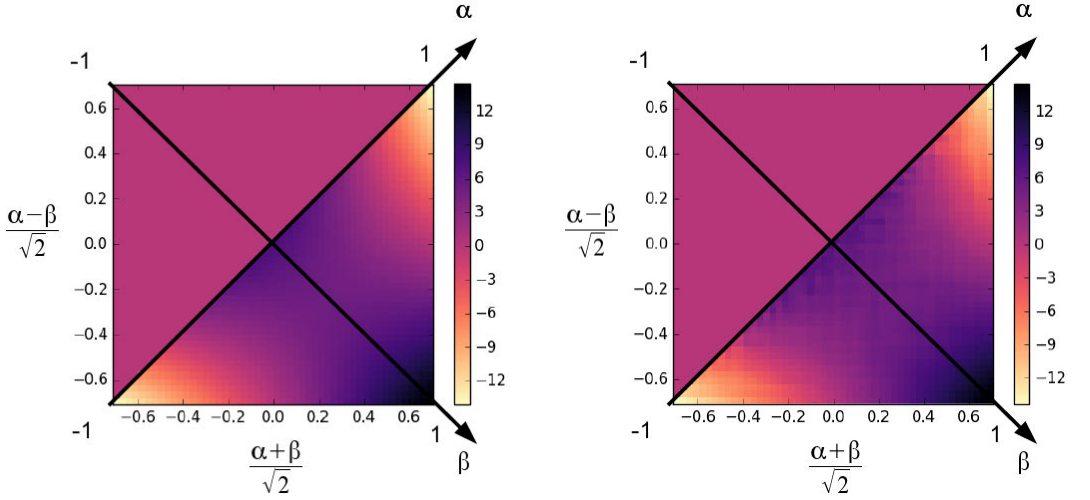


**Figure 4.** Left: Pion valence dressed-quark overlap GPD at  $t = 0$  analytically computed from the DD in Eq. (16) in the Pobylitsa gauge. Right: Pion valence dressed-quark overlap GPD at  $t = 0$  numerically computed from the DD resulting of the numerical Radon transform of the GPD restricted to the DGLAP region. The support for the parameters  $(\beta, \alpha)$  corresponds to a  $\pi/2$ -rotated square with the two combinations  $(\alpha + \beta)/\sqrt{2}$  and  $(\alpha - \beta)/\sqrt{2}$  for the horizontal and vertical axes.

requires some flexible tools to design, try and identify the optimal numerical methods. The large number of possibly involved distributions requires a multichannel analysis to constrain GPDs from different experimental data. The foreseen accuracy of experimental data to be measured at Jefferson Lab or at COMPASS requires the careful design of tools to meet the challenge of the high-precision era, to be able to make the best from experimental data, and to create new sophisticated and realistic GPD models. The same tools should also be used *e.g.* to contribute to the physics case of a future Electron Ion Collider (EIC). Integrating these tools in one single platform for the theory and phenomenology of GPDs is the aim of the PARTONS (PARTonic Tomography Of Nucleon Software) project [34].

## 5.1 Computing chain

Fig. 5 gives the general structure of the PARTONS framework. Although only GPDs and the DVCS channel have been integrated so far, the architecture should be flexible enough to deal with any process that can be factorized in short and large distance contributions.

## 5.2 Example

The PARTONS framework is written in C++, but a lot of attention has been paid to automation features. It is possible to perform computations with PARTONS without writing a single line of C++ by using *computing scenarios*: a simple XML file containing the computation configuration (perturbative QCD hypothesis, GPD model, etc.) and the kinematics of interest can be used to compute any GPD-related quantity, from GPDs themselves to observables.

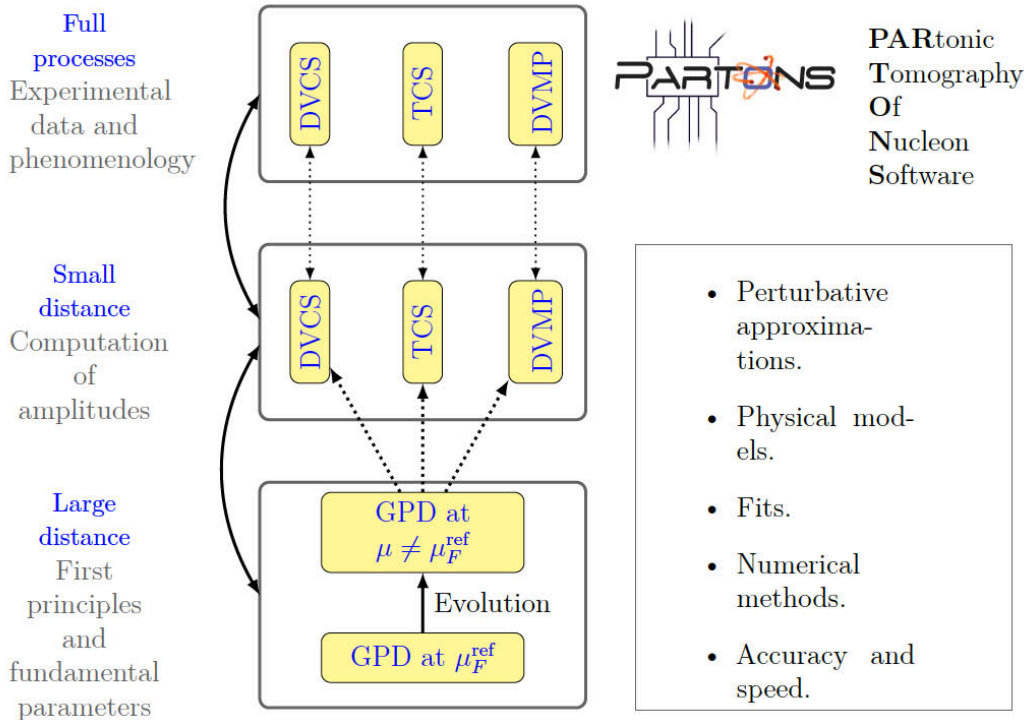


**Figure 5.** The architecture of the PARTONS code is designed to compute observables related to processes that can be factorized in short and large distance contributions.

The code below gives an example of the computation of a Compton Form Factor (CFF) at LO. Each line of code corresponds to a physical hypothesis. Work is in progress to invert the Radon transform and build generic GPD models within PARTONS in a similar way. Such GPD models would immediately be ready for phenomenological studies and comparisons to experimental data thanks to the other components of the PARTONS framework.

```

1 <?xml version="1.0" encoding="UTF-8" standalone="yes" ?>
2 <scenario date="2016-08-28"
3   description="Computing_a_convolution_coefficient_from_a_GPD_model">
4   <task service="ConvolCoeffFunctionService" method="computeWithGPDModel">
5     <kinematics type="DVCSConvolCoeffFunctionKinematic">
6       <param name="xi" value="0.5" />
7       <param name="t" value="-0.1346" />
8       <param name="Q2" value="1.5557" />
9       <param name="MuF2" value="4" />
10      <param name="MuR2" value="4" />
11    </kinematics>
12    <computation_configuration>
13      <module type="GPDModule">
14        <param name="className" value="GK11Model" />
15      </module>
16      <module type="DVCSConvolCoeffFunctionModule">
17        <param name="className" value="DVCSCFModel" />
18        <param name="qcd_order_type" value="LO" />
19      </module>
20    </computation_configuration>
21  </task>
22 </scenario>

```

## 6 Conclusions

We have shown how the positivity and polynomiality constraints can be consistently implemented. Although we illustrated our approach through an example from Dyson-Schwinger equations, where we can additionally implement chiral symmetry breaking in consistent way, it should be emphasized that this modeling strategy is completely general and is not tied to a specific family of models. In that respect we propose a systematic procedure to construct models of Generalized Parton Distributions from any "reasonable" Ansatz of Light Front Wave Functions. The scientific computing aspects of this problem are naturally treated in the framework PARTONS which has been designed for phenomenology and theory purposes.

## Acknowledgements

This work has been partially supported by Spanish ministry projects FPA-2014-53631-C2-2-P, French GDR 3753 QCD "Chromodynamique Quantique" and ANR-12-MONU-0008-01 "PARTONS" and U.S. Department of Energy, Office of Science, Office of Nuclear Physics, under contract no. DE-AC02-06CH11357.

## References

- [1] D. Mueller, D. Robaschik, B. Geyer, F. Dittes, J. Hořejši, Fortsch.Phys. **42**, 101 (1994), [hep-ph/9812448](#)
- [2] X.D. Ji, Phys.Rev. **D55**, 7114 (1997), [hep-ph/9609381](#)
- [3] A. Radyushkin, Phys.Rev. **D56**, 5524 (1997), [hep-ph/9704207](#)
- [4] N.G. Stefanis, C. Alexandrou, T. Horn, H. Moutarde, I. Scimemi (2016), [1612.03077](#)
- [5] X.D. Ji, J.Phys. **G24**, 1181 (1998), [hep-ph/9807358](#)
- [6] K. Goeke, M.V. Polyakov, M. Vanderhaeghen, Prog.Part.Nucl.Phys. **47**, 401 (2001), [hep-ph/0106012](#)
- [7] M. Diehl, Phys.Rept. **388**, 41 (2003), [hep-ph/0307382](#)
- [8] A. Belitsky, A. Radyushkin, Phys.Rept. **418**, 1 (2005), [hep-ph/0504030](#)
- [9] S. Boffi, B. Pasquini, Riv.Nuovo Cim. **30**, 387 (2007), [0711.2625](#)
- [10] M. Guidal, H. Moutarde, M. Vanderhaeghen, Rept.Prog.Phys. **76**, 066202 (2013), [1303.6600](#)
- [11] D. Mueller, Few Body Syst. **55**, 317 (2014), [1405.2817](#)
- [12] L. Favart, M. Guidal, T. Horn, P. Kroll, Eur. Phys. J. **A52**, 158 (2016), [1511.04535](#)
- [13] K. Kumericki, S. Liuti, H. Moutarde, Eur. Phys. J. **A52**, 157 (2016), [1602.02763](#)
- [14] N. d'Hose, S. Niccolai, A. Rostomyan, Eur. Phys. J. **A52**, 151 (2016)
- [15] A. Radyushkin, Phys.Rev. **D59**, 014030 (1999), [hep-ph/9805342](#)
- [16] A. Radyushkin, Phys.Lett. **B449**, 81 (1999), [hep-ph/9810466](#)
- [17] O. Teryaev, Phys.Lett. **B510**, 125 (2001), [hep-ph/0102303](#)
- [18] C. Mezrag, H. Moutarde, J. Rodriguez-Quintero, Few Body Syst. **57**, 729 (2016), [1602.07722](#)
- [19] A. Hertle, Mathematische Zeitschrift **184**, 165 (1983)

- [20] P.V. Pobylitsa, Phys. Rev. **D66**, 094002 (2002), [hep-ph/0204337](#)
- [21] M. Diehl, T. Feldmann, R. Jakob, P. Kroll, Nucl. Phys. **B596**, 33 (2001), [Erratum: Nucl. Phys.B605,647(2001)], [hep-ph/0009255](#)
- [22] D.S. Hwang, D. Mueller, Phys. Lett. **B660**, 350 (2008), [0710.1567](#)
- [23] D. Müller, D.S. Hwang (2014), [1407.1655](#)
- [24] C. Mezrag, L. Chang, H. Moutarde, C.D. Roberts, J. Rodríguez-Quintero, F. Sabatié, S.M. Schmidt, Phys. Lett. **B741**, 190 (2014), [1411.6634](#)
- [25] L. Chang, I. Cloet, J. Cobos-Martinez, C. Roberts, S. Schmidt et al., Phys.Rev.Lett. **110**, 132001 (2013), [1301.0324](#)
- [26] L. Chang, C. Mezrag, H. Moutarde, C.D. Roberts, J. Rodríguez-Quintero, P.C. Tandy, Phys. Lett. **B737**, 23 (2014), [1406.5450](#)
- [27] C. Mezrag, H. Moutarde, J. Rodríguez-Quintero, F. Sabatié (2014), [1406.7425](#)
- [28] A.V. Belitsky, D. Mueller, A. Kirchner, A. Schafer, Phys. Rev. **D64**, 116002 (2001), [hep-ph/0011314](#)
- [29] P.V. Pobylitsa, Phys. Rev. **D70**, 034004 (2004), [hep-ph/0211160](#)
- [30] B. Tiburzi, Phys.Rev. **D70**, 057504 (2004), [hep-ph/0405211](#)
- [31] H. Moutarde, Habilitation thesis. To be published (2017)
- [32] N. Chouika, *et al.*, Work in progress (2017)
- [33] I. Musatov, A. Radyushkin, Phys.Rev. **D61**, 074027 (2000), [hep-ph/9905376](#)
- [34] B. Berthou, D. Binosi, N. Chouika, M. Guidal, C. Mezrag, H. Moutarde, F. Sabatié, P. Sznajder, J. Wagner (2015), [1512.06174](#)